Mapping and investigation of lunar wrinkle ridges in Mare Serenitatis.

Lennard Pauw[1], H. Hiesinger[1], C. H. van der Bogert[1] and T. Früh[1], [1]Institut für Planetologie, Westfälische Wilhelms-Universität Münster, Wilhelm-Klemm-Str.10, 48149 Münster, Germany, (l_pauw01@uni-muenster.de).

Introduction: With modern high-resolution imagery and topographic data, distinctive structures like wrinkle ridges or lobate scarps are observed, to provide insights into regional as well as global geological processes at the lunar surface. This work deals particularly with wrinkle ridges in Mare Serenitatis. Wrinkle ridges are linear or sinuous positive topographic features, preferentially found in maria basins or lowland- and plain-areas, consisting of a broad arch and a superposed sharper ridge [1-4]. It is agreed upon that they are contractional features formed by a combination of folding and thrust faulting in response to compressional stresses [2,4-8]. Wrinkle ridges are typically oriented both radial and concentric within mare basins [2,18] and deform the oldest and youngest mare basalts, implying an extended period of localized crustal shortening [2,4]. Mare Serenitatis is considered as a mascon-related multi-ring impact basin with pre-mare topography similar to the topography of Mare Orientale [9,10]. In accordance with Head's (1979) [10] reconstruction of the Serenitatis ring system and Yue's (2017) [18] global survey of lunar wrinkle ridges, we selected and mapped wrinkle ridges and coherent wrinkle ridge structures within the mare, to compare morphologies and boulder field frequencies, in order to investigate possible modifications and reactivations by tectonic processes.

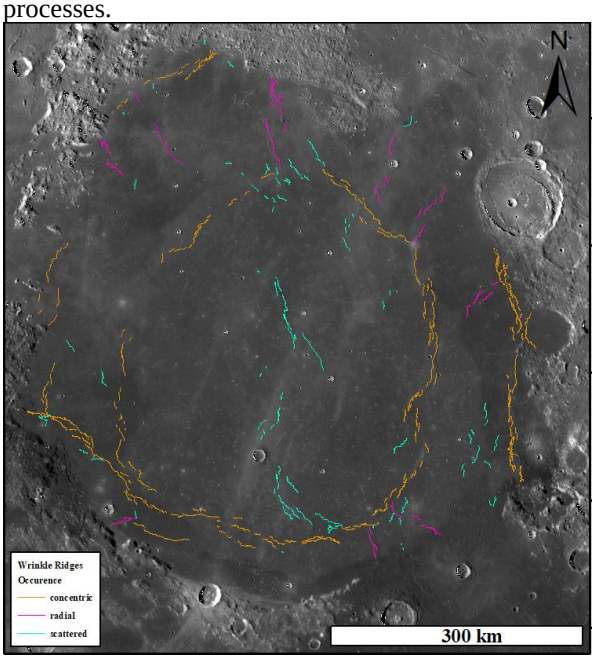

Figure 1: WAC image of mapped wrinkle ridges in Mare Serenitatis, based on their orientation-class.

Data and Methods: We used TC (Terrain Camera; 10 m/pixel) image data provided by the Kaguya spacecraft (SELENE), NAC and WAC imagery provided by the Lunar Reconnaissance Orbiter (LRO), and merged topographic data (SLDEM2015) from the Terrain Camera (TC) and Lunar Orbiter Laser Altimeter (LOLA), as an unprecedented dataset for identifying and classifying wrinkle ridges. These data were imported into ArcGIS and with the help of tools like hill shading and slope maps, we selected over 470 wrinkle ridges and eventually mapped them on the basis of their orientations, lengths, appearances, and distributions of boulder fields. Furthermore, we divided them into primary and secondary ridges. Secondary wrinkle ridges are known to commonly flank or cap larger primary ridges [19] and show very small impact on local topography. We additionally assigned all wrinkle ridges with an identification number (ID), so one can compare individual wrinkle ridges, wrinkle ridge clusters or coherent wrinkle ridge systems and discuss their individual properties.

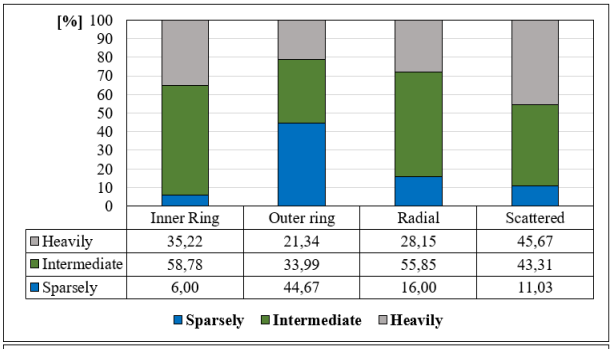

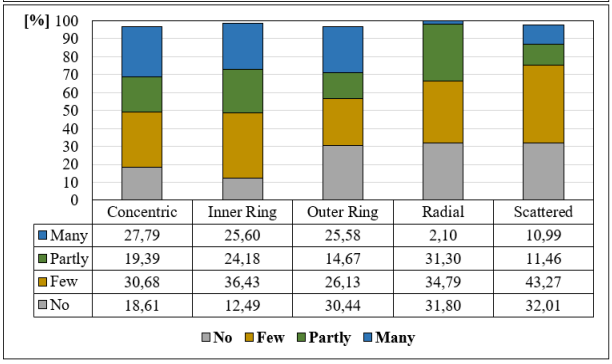

Figure 2: The first diagram shows degradation states by orientation. The second diagram includes the distribution of boulder fields by orientation. Both diagrams relate to the total length of mapped wrinkle ridges in Mare Serenitatis.

Results: Wrinkle ridges were mainly classified by their orientation, degradation/morphology, and boulder field distribution. We divided them by their orientation, resulting in an inner ring system (Linné Ring), an outer ring system in proximity to Ring Haemus, a radial, and a scattered group. The length of wrinkle ridges was determined for each individual class and normalized to the total length of wrinkle ridges in Mare Serenitatis. About 61 % of the mapped wrinkle ridges in Mare Serenitatis occur concentric with a mean length of 11.03 km, ~24 % are scattered with an average length of 12.73 km, and ~15 % are radial oriented, having a mean length of 9.63 km. Considering this, the inner ring system displays ~30 % of the total wrinkle ridge length in Mare Serenitatis, while ~21 % can be associated with the outer ring system. Further results show that the inner ring system appears morphologically more heavily degraded than the outer ring system (Fig. 2.1). About 45 % of the wrinkle ridges associated with the outer ring are sparsely degraded and display crisp morphologies, whereas the inner ring consists of only 6 % sparsely degraded wrinkle ridges and higher values for the heavily and intermediate degraded ridges. At the same time, the inner ring system shows higher boulder field frequencies of ~20 %, when adding up all boulder field classes, distributed along and on top of its wrinkle ridges (Fig. 2.2). The boulder field distribution and frequency was classified as: not existent, few, partly and many boulder fields. These are relative assessments solely related to wrinkle ridges in Mare Serenitatis. Overall, concentric wrinkle ridges are generally ~13 % more frequented by boulder fields than radial or scattered oriented ridges.

Discussion: Based on small scale, crisp appearances and crosscutting relations with small-diameter craters, sparsely degraded wrinkle ridges are considered to be younger than more heavily degraded wrinkle ridges that deform mare basalts with ages of ~3.0-3.8 Ga [11,12]. The occurrence of boulders associated with wrinkle ridges, and the boulder field areas along a ridge can be related to recent activities [13-15]. Additionally, blocky fields and patches on low-slope surfaces requires ongoing processes that continuously expose the substrates [13,14]. High reflectance material in close proximity to wrinkle ridge boulders likely represents freshly exposed rock and soil [14]. With that in mind, the inner ring system appears older and more heavily degraded while showing higher boulder field frequencies than the outer ring system. Coherent structures in the basins interior have different distributions and frequencies of boulder fields that may be an indicator for recent activities or reactivations of tectonic features [13]. This would suggest, that despite super-isotropic stresses, like mascon tectonics [9,10], interpreted as contractional stresses resulting from basin loading with mare basalts [13,16], wrinkle ridges in Mare Serenitatis seem to, at least to some degree, also reflect non-isotropic stresses.

Conclusion: The results suggest an extended time for the formation or modification of coherent wrinkle ridges in Serenitatis based on their morphology, and an independent reactivation of isolated ridge systems, based on their boulder field abundances. This would indicate that beyond mascon tectonics, different stress fields, possibly induced by lunar nearside tectonics, could lead to reactivations of geological features like isolated wrinkle ridge structures and ring systems in Mare Serenitatis. In regard to these nearside activities, different hypotheses, e.g., the influence of tidal stresses [20] or active nearside tectonic systems (ANTS) related to deep transient generated stress systems [13,17], are currently discussed. The results of this study display very complex and spatially heterogeneous distributions of stress fields that affected or could possibly still affect lunar wrinkle ridges in Mare Serenitatis.

Acknowledgments: I acknowledge the use of data downloaded from the Planetary Data System (PDS; https://pds.nasa.gov/), SELENE data archive (DARTS; https://darts.isas.jaxa.jp/), and imagery from Lunar QuickMap (https://quickmap.lroc.asu.edu/) to generate parts of the results shown in this abstract.

References: [1] Strom (1972) The Moon 47, 187–215. [2] Maxwell et al. (1975) GSA Bulletin 86, 1273-1278. [3] Plescia and Golombek (1986) GSA Bulletin 97, 1289-1299. [4] Watters and Johnson (2010) Planetary Tectonics, 121- 182. [5] Sharpton and Head (1988) Proc. LPSC 18, 307-317. [6] Schultz (2000) JGR 105, 12035-12052. [7] Watters (1992) Geology 20, 609–612. [8] Ono et al. (2009) Science 323, 909-912. [9] Spudis (2009) The Geology of Multi-Ring Impact Basins, 18-41. [10] Head (1979) The Moon and the Planets 21, 439-462. [11] Wilhelms et al. (1987) USGS, 283-292. [12] Hiesinger et al. (2000) JGR 105, 29239– 29275. [13] Valantinas and Schultz (2020) Geology 48, 649-653. [14] French et al. (2019) JGR 124, 2970-2982. [15] Lu et al. (2019) Icarus 329, 24-33. [16] Watters (2019) Nature Geoscience 12, 411-417. [17] Schultz and Crawford (2011), GSA Bulletin 477, 141-159. [18] Yue et al. (2017) EPSL 477, 14-20. [19] Watters (1988) JGR 93, 236-254. [20] Watters et al. (2015) Geology 43, 851-854.